Hamiltonian Simulation of Ideal Fluids

Martin Pujol[1], Thibault Fredon[2], Marc Brachet[3], Fabrice Debbasch[4], Julien Zylberman[1]

[1]CERFACS, European Center for Research and Advanced Training in Scientific Computing, Toulouse, France
[2]Plasma Science and Fusion Center, Massachusetts Institute of Technology, Cambridge, USA
[3]Sorbonne Universite, Observatoire de Paris, Paris, France
[4]Laboratoire de Physique de l'Ecole Normale Supérieure, Paris, France

November 13, 2026

Section 1

Quantum Computing

I. Qubit: The Quantum Bit

A qubit is a normalized vector in $\mathbb{C}^2$:

$$\boxed{|\psi\rangle = \alpha|0\rangle + \beta|1\rangle, \qquad |\alpha|^2 + |\beta|^2 = 1}$$

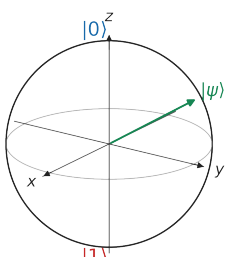
I. Qubit: The Quantum Bit

A qubit is a normalized vector in $\mathbb{C}^2$:

$$|\psi\rangle = \alpha|0\rangle + \beta|1\rangle, \qquad |\alpha|^2 + |\beta|^2 = 1$$

Elementary quantum gates act on qubits as rotations.

$|\psi\rangle$ —



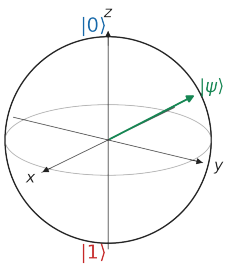
I. Qubit: The Quantum Bit

A qubit is a normalized vector in $\mathbb{C}^2$:

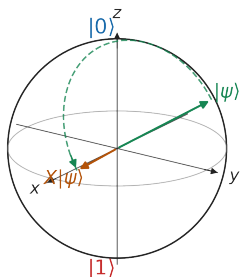
$$|\psi\rangle = \alpha|0\rangle + \beta|1\rangle, \qquad |\alpha|^2 + |\beta|^2 = 1$$

Elementary quantum gates act on qubits as rotations.

$|\psi\rangle$ —



$|\psi\rangle$ — X —

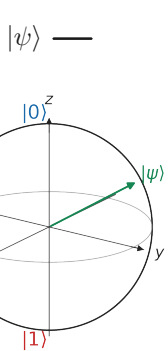


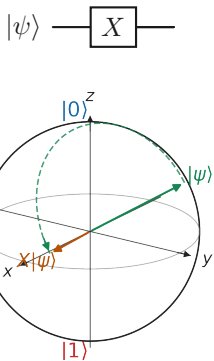
I. Qubit: The Quantum Bit

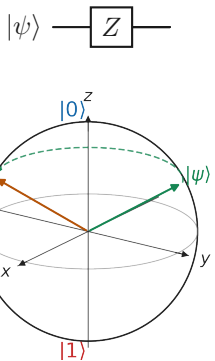
A qubit is a normalized vector in $\mathbb{C}^2$:

$$|\psi\rangle = \alpha|0\rangle + \beta|1\rangle, \qquad |\alpha|^2 + |\beta|^2 = 1$$

Elementary quantum gates act on qubits as rotations.







II. Tensor Product: Many-Qubit Systems

Two qubits are described by the tensor product:

$$|\psi\rangle \otimes |\phi\rangle = (\alpha|0\rangle + \beta|1\rangle) \otimes (\gamma|0\rangle + \delta|1\rangle).$$
$$= \alpha\gamma|00\rangle + \alpha\delta|01\rangle + \beta\gamma|10\rangle + \beta\delta|11\rangle.$$

II. Tensor Product: Many-Qubit Systems

Two qubits are described by the tensor product:

$$|\psi\rangle \otimes |\phi\rangle = (\alpha|0\rangle + \beta|1\rangle) \otimes (\gamma|0\rangle + \delta|1\rangle).$$
$$= \alpha\gamma|00\rangle + \alpha\delta|01\rangle + \beta\gamma|10\rangle + \beta\delta|11\rangle.$$

$$\boxed{\mathbb{C}^2 \otimes \mathbb{C}^2 \simeq \mathbb{C}^4}$$

$$\begin{pmatrix} \alpha \\ \beta \end{pmatrix} \otimes \begin{pmatrix} \gamma \\ \delta \end{pmatrix} = \begin{pmatrix} \alpha\gamma \\ \alpha\delta \\ \beta\gamma \\ \beta\delta \end{pmatrix}$$

II. Tensor Product: Many-Qubit Systems

Two qubits are described by the tensor product:

$$|\psi\rangle \otimes |\phi\rangle = (\alpha|0\rangle + \beta|1\rangle) \otimes (\gamma|0\rangle + \delta|1\rangle).$$
$$= \alpha\gamma|00\rangle + \alpha\delta|01\rangle + \beta\gamma|10\rangle + \beta\delta|11\rangle.$$

$$\boxed{\mathbb{C}^2 \otimes \mathbb{C}^2 \simeq \mathbb{C}^4}$$

$$\begin{pmatrix} \alpha \\ \beta \end{pmatrix} \otimes \begin{pmatrix} \gamma \\ \delta \end{pmatrix} = \begin{pmatrix} \alpha\gamma \\ \alpha\delta \\ \beta\gamma \\ \beta\delta \end{pmatrix}$$

$$\boxed{\underbrace{\mathbb{C}^2 \otimes \cdots \otimes \mathbb{C}^2}_{n \text{ qubits}} \simeq \mathbb{C}^{2^n}}$$

III. Entanglement

Product state:

$$|\psi\rangle = |\psi_1\rangle \otimes |\psi_2\rangle.$$

III. Entanglement

Product state:

$$|\psi\rangle = |\psi_1\rangle \otimes |\psi_2\rangle.$$

Entangled state:

$$\boxed{|\Phi^+\rangle = \frac{|00\rangle + |11\rangle}{\sqrt{2}}}$$

cannot be factorized.

III. Entanglement

Product state:

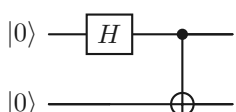
$$|\psi\rangle = |\psi_1\rangle \otimes |\psi_2\rangle.$$

Entangled state:

$$\boxed{|\Phi^+\rangle = \frac{|00\rangle + |11\rangle}{\sqrt{2}}}$$

cannot be factorized.

Creating entanglement with a quantum circuit



III. Entanglement

Product state:

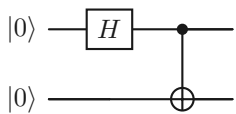
$$|\psi\rangle = |\psi_1\rangle \otimes |\psi_2\rangle.$$

Entangled state:

$$\boxed{|\Phi^+\rangle = \frac{|00\rangle + |11\rangle}{\sqrt{2}}}$$

cannot be factorized.

Creating entanglement with a quantum circuit



$$|00\rangle \xrightarrow{H\otimes I} \frac{|00\rangle + |10\rangle}{\sqrt{2}} \xrightarrow{\text{CNOT}} \boxed{\frac{|00\rangle + |11\rangle}{\sqrt{2}}}$$

III. Entanglement

Product state:

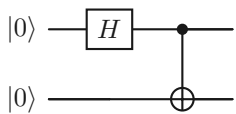
$$|\psi\rangle = |\psi_1\rangle \otimes |\psi_2\rangle.$$

Entangled state:

$$\boxed{|\Phi^+\rangle = \frac{|00\rangle + |11\rangle}{\sqrt{2}}}$$

cannot be factorized.

Creating entanglement with a quantum circuit



$$|00\rangle \xrightarrow{H\otimes I} \frac{|00\rangle + |10\rangle}{\sqrt{2}} \xrightarrow{\text{CNOT}} \boxed{\frac{|00\rangle + |11\rangle}{\sqrt{2}}}$$

IV. Quantum Measurement

A general n-qubit state is

$$|\psi\rangle = \sum_{x=0}^{2^n-1} c_x |x\rangle, \qquad \sum_x |c_x|^2 = 1.$$

IV. Quantum Measurement

A general n-qubit state is

$$|\psi\rangle = \sum_{x=0}^{2^n-1} c_x |x\rangle, \qquad \sum_x |c_x|^2 = 1.$$

Born's rule:

$$\boxed{P(x) = |\langle x|\psi\rangle|^2 = |c_x|^2}$$

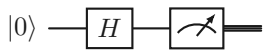
IV. Quantum Measurement

A general n-qubit state is

$$|\psi\rangle = \sum_{x=0}^{2^n-1} c_x |x\rangle, \qquad \sum_x |c_x|^2 = 1.$$

Born's rule:

$$\boxed{P(x) = |\langle x|\psi\rangle|^2 = |c_x|^2}$$



$$P(0) = P(1) = \frac{1}{2}$$

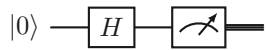
IV. Quantum Measurement

A general n-qubit state is

$$|\psi\rangle = \sum_{x=0}^{2^n-1} c_x |x\rangle, \qquad \sum_x |c_x|^2 = 1.$$

Born's rule:

$$\boxed{P(x) = |\langle x|\psi\rangle|^2 = |c_x|^2}$$



$$P(0) = P(1) = \frac{1}{2}$$

- A quantum computer applies **unitary matrices** to vectors in an exponentially large Hilbert space.
- These matrices are implemented through **local operations**: one- and two-qubit gates.
- Measurement produces a **classical outcome**, sampled according to Born's rule.

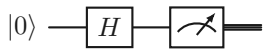
IV. Quantum Measurement

A general n-qubit state is

$$|\psi\rangle = \sum_{x=0}^{2^n-1} c_x |x\rangle, \qquad \sum_x |c_x|^2 = 1.$$

Born's rule:

$$\boxed{P(x) = |\langle x|\psi\rangle|^2 = |c_x|^2}$$



$$P(0) = P(1) = \frac{1}{2}$$

- A quantum computer applies **unitary matrices** to vectors in an exponentially large Hilbert space.
- These matrices are implemented through **local operations**: one- and two-qubit gates.
- Measurement produces a **classical outcome**, sampled according to Born's rule.

Exponential state-space dimension does not imply exponential information readout.

Section 2

Problem Statement

The computational challenge

- **High Reynolds numbers** $\Rightarrow$ increasingly fine structures.
- **Turbulence couples a wide range of scales**, from large eddies down to the smallest structures.
- **Direct numerical simulation** must resolve all these scales.

Higher Reynolds numbers require better representations.

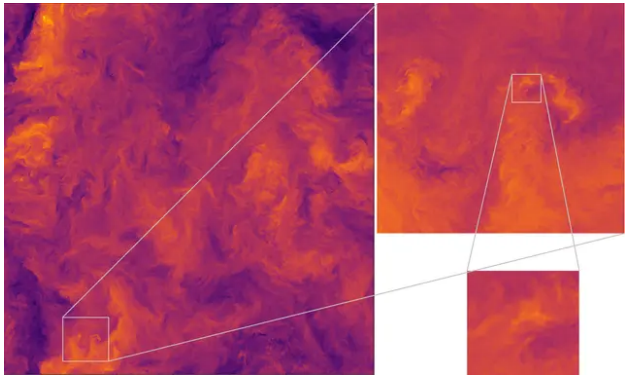


Figure 1: Homogeneous isotropic turbulence DNS, 8192^3 grid, $Re_\lambda \simeq 1200$, JHTDB / Georgia Tech.

Computed on **262 144 CPU cores** on Blue Waters

Nonlinear dynamics on Quantum Computer

Fluid dynamics

$$\partial_t \vec{u} + \vec{u} \cdot \nabla \vec{u} = -\nabla p + \mu \Delta \vec{u}$$

Nonlinear



Quantum evolution

$$|\psi(t)\rangle = e^{-iHt}|\psi(0)\rangle$$

Linear & unitary

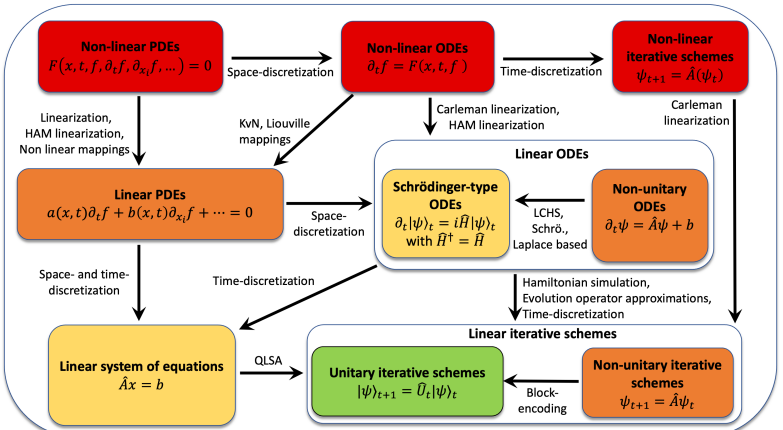


Figure 2: Different approaches to solving nonlinear PDEs on a quantum computer. Adapted from J. Zylberman's PhD thesis (2025).

Fluids

2D Navier–Stokes (no forcing)

$$\boxed{\partial_t \vec{u} + \vec{u} \cdot \nabla \vec{u} = -\nabla p + \nu \nabla^2 \vec{u}, \qquad \nabla \cdot \vec{u} = 0}$$

Fluids

2D Navier–Stokes (no forcing)

$$\boxed{\partial_t \vec{u} + \vec{u} \cdot \nabla \vec{u} = -\nabla p + \nu \nabla^2 \vec{u}, \qquad \nabla \cdot \vec{u} = 0}$$

Symmetry reduction: incompressibility eliminates the pressure

$$\nabla \cdot \mathbf{u} = 0 \;\rightarrow\; \mathbf{u} = \mathbf{e}_z \times \nabla \phi, \qquad \omega = \nabla^2 \phi$$

Vorticity formulation

$$\partial_t \omega = -\{\phi, \omega\} + \nu \nabla^2 \omega, \qquad \{\phi, \omega\} = \partial_x \phi \, \partial_y \omega - \partial_x \omega \, \partial_y \phi$$

Fluids

2D Navier–Stokes (no forcing)

$$\boxed{\partial_t \vec{u} + \vec{u} \cdot \nabla \vec{u} = -\nabla p + \nu \nabla^2 \vec{u}, \qquad \nabla \cdot \vec{u} = 0}$$

Symmetry reduction: incompressibility eliminates the pressure

$$\nabla \cdot \mathbf{u} = 0 \;\rightarrow\; \mathbf{u} = \mathbf{e}_z \times \nabla \phi, \qquad \omega = \nabla^2 \phi$$

Vorticity formulation

$$\partial_t \omega = -\{\phi, \omega\} + \nu \nabla^2 \omega, \qquad \{\phi, \omega\} = \partial_x \phi \, \partial_y \omega - \partial_x \omega \, \partial_y \phi$$

Viscous fluid $(\nu > 0)$ — dissipates $\xrightarrow{\nu \to 0}$ **Ideal fluid** — conserves

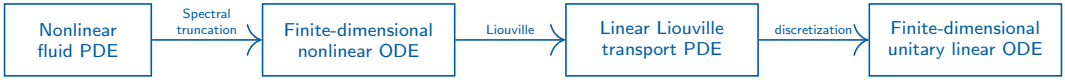
$$\dot{E} = -\nu \int \omega^2 \, d\mathbf{x}, \qquad \dot{\Omega} = -\nu \int |\nabla \omega|^2 \, d\mathbf{x}$$

$$\boxed{E = \frac{1}{2} \int |\mathbf{u}|^2 \, d\mathbf{x}, \qquad \Omega = \frac{1}{2} \int \omega^2 \, d\mathbf{x}}$$

- Rapid generation of fine-scale structures
- Conservation of energy and enstrophy $\Rightarrow$ existence and smoothness guaranteed

Section 3

Liouville Embedding



Spectral truncation



Expand the vorticity field on $\mathbb{T}^2$: $\omega^M(\mathbf{x},t) = \sqrt{\frac{2}{V}} \sum_{|\mathbf{k}|<M} \left[a_{\mathbf{k}}(t)\ \cos(\mathbf{k}\cdot\mathbf{x}) + b_{\mathbf{k}}(t)\sin(\mathbf{k}\cdot\mathbf{x})\right]$

Spectral truncation



Expand the vorticity field on $\mathbb{T}^2$: $\omega^M(\mathbf{x},t) = \sqrt{\frac{2}{V}} \sum_{|\mathbf{k}|<M} \left[a_{\mathbf{k}}(t)\ \cos(\mathbf{k}\cdot\mathbf{x}) + b_{\mathbf{k}}(t)\sin(\mathbf{k}\cdot\mathbf{x})\right]$

$$\boldsymbol{\phi} = \begin{pmatrix} a_{(0,-N)} \\ \vdots \\ a_{(N,N)} \\ b_{(0,-N)} \\ \vdots \\ b_{(N,N)} \end{pmatrix} \longrightarrow \boxed{\dot{\phi}_\alpha = f_\alpha(\phi) = \sum_{\beta,\gamma=1}^{D} C_{\alpha\beta\gamma}\,\phi_\beta\phi_\gamma}$$

Spectrally truncated Euler equations

Spectral truncation



Expand the vorticity field on $\mathbb{T}^2$: $\omega^M(\mathbf{x},t) = \sqrt{\frac{2}{V}} \sum_{|\mathbf{k}|<M} \left[a_{\mathbf{k}}(t)\ \cos(\mathbf{k}\cdot\mathbf{x}) + b_{\mathbf{k}}(t)\sin(\mathbf{k}\cdot\mathbf{x})\right]$

$$\boldsymbol{\phi} = \begin{pmatrix} a_{(0,-N)} \\ \vdots \\ a_{(N,N)} \\ b_{(0,-N)} \\ \vdots \\ b_{(N,N)} \end{pmatrix} \longrightarrow \boxed{\dot{\phi}_\alpha = f_\alpha(\phi) = \sum_{\beta,\gamma=1}^{D} C_{\alpha\beta\gamma}\,\phi_\beta\phi_\gamma}$$

Spectrally truncated Euler equations

The spectral truncation preserve structure !

- Similar decomposition for other ideal fluids:

$$\dot{E} = \sum_{\alpha,\beta,\gamma} C_{\alpha\beta\gamma}\phi_\alpha\phi_\beta\phi_\gamma = 0$$

$$\underbrace{\nabla\cdot f = \sum_{\alpha,\beta} \left(C_{\alpha\alpha\beta} + C_{\alpha\beta\alpha}\right)\phi_\beta = 0}_{\text{Phase-space volume conservation}}$$

Spectral truncation



Expand the vorticity field on $\mathbb{T}^2$: $\omega^M(\mathbf{x},t) = \sqrt{\frac{2}{V}} \sum_{|\mathbf{k}|<M} \left[a_{\mathbf{k}}(t)\ \cos(\mathbf{k}\cdot\mathbf{x}) + b_{\mathbf{k}}(t) \sin(\mathbf{k}\cdot\mathbf{x}) \right]$

$$\boldsymbol{\phi} = \begin{pmatrix} a_{(0,-N)} \\ \vdots \\ a_{(N,N)} \\ b_{(0,-N)} \\ \vdots \\ b_{(N,N)} \end{pmatrix} \longrightarrow \boxed{\dot{\phi}_\alpha = f_\alpha(\phi) = \sum_{\beta,\gamma=1}^{D} C_{\alpha\beta\gamma}\, \phi_\beta \phi_\gamma}$$

Spectrally truncated Euler equations

The spectral truncation preserve structure !

- Similar decomposition for other ideal fluids:

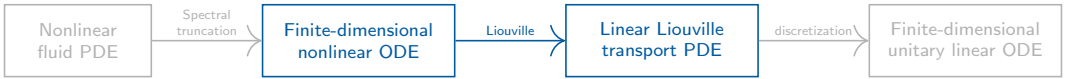
$$\dot{E} = \sum_{\alpha,\beta,\gamma} C_{\alpha\beta\gamma}\phi_\alpha\phi_\beta\phi_\gamma = 0$$

$$\underbrace{\nabla \cdot f = \sum_{\alpha,\beta} \left(C_{\alpha\alpha\beta} + C_{\alpha\beta\alpha}\right) \phi_\beta = 0}_{\text{Phase-space volume conservation}}$$

- **Stronger condition:** (Inherited from field incompressibility)

$$\boxed{\frac{\partial f_\alpha}{\partial \phi_\alpha} = \sum_\gamma \left(\overbrace{C_{\alpha\alpha\gamma}}^{\text{antisymmetry}} + \overbrace{C_{\alpha\gamma\alpha}}^{(\vec{\varphi}_\alpha\cdot\nabla)\vec{\varphi}_\alpha=0} \right) \phi_\gamma = 0 \qquad \forall\alpha.}$$

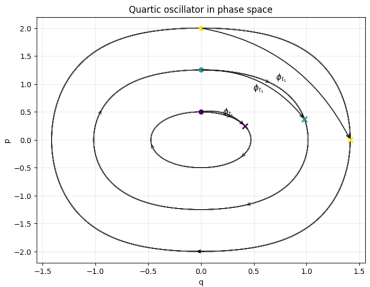
Liouville embedding



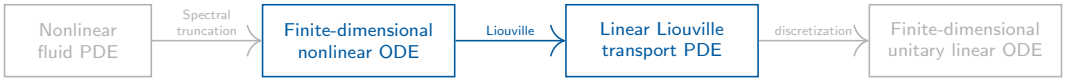
From a point $\phi \in \mathbb{R}^D$

$$\dot{\phi}_\alpha = \sum_{\beta,\gamma=1}^{D} C_{\alpha\beta\gamma}\,\phi_\beta\phi_\gamma$$

Non-Linear ODE



Liouville embedding



From a point $\phi \in \mathbb{R}^D$

$$\dot{\phi}_\alpha = \sum_{\beta,\gamma=1}^{D} C_{\alpha\beta\gamma}\,\phi_\beta\phi_\gamma$$

Non-Linear ODE

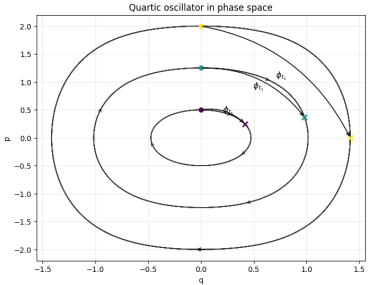
$\nabla\cdot f=0$

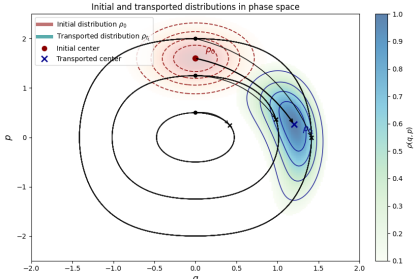
Liouville theorem

To a distribution $\rho \in C(\mathbb{R}^D)$

$$\partial_t \rho_t(\phi) = -\sum_\alpha f_\alpha(\phi)\,\partial_\alpha \rho_t(\phi)$$

Linear PDE



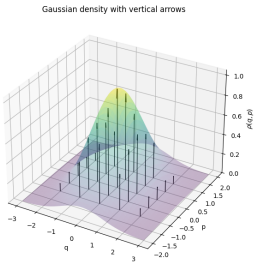


Discretization of the phase-space



$N = 2^n$ grid points per axis, D axes $\Rightarrow$ nD qubits

$$\rho(\boldsymbol{\phi}) \longmapsto |\rho\rangle = \sum_{\phi_1,\ldots,\phi_D} \frac{\rho(\boldsymbol{\phi})}{\|\rho\|} |\phi_1,\ldots,\phi_D\rangle$$



Discretization of the phase-space



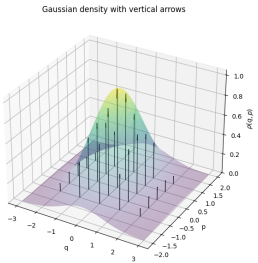
$N = 2^n$ grid points per axis, D axes $\Rightarrow nD$ qubits

$$\partial_{\phi_\alpha} \longrightarrow \hat{\partial}_\alpha = \frac{1}{\Delta x_\alpha} \sum_{k=-p}^{p} a_k \, \hat{S}_\alpha^{k} \; {}^{*}$$

$$\rho(\boldsymbol{\phi}) \longmapsto |\rho\rangle = \sum_{\phi_1,\ldots,\phi_D} \frac{\rho(\boldsymbol{\phi})}{\|\rho\|} |\phi_1,\ldots,\phi_D\rangle$$

$$\hat{S}_\alpha^{k} |\phi_1,\ldots,\phi_\alpha,\ldots,\phi_D\rangle = |\phi_1,\ldots,\phi_\alpha + k\Delta x_\alpha,\ldots,\phi_D\rangle$$

* finite differences with periodic boundary conditions, error $O(\Delta x_\alpha^{2p})$

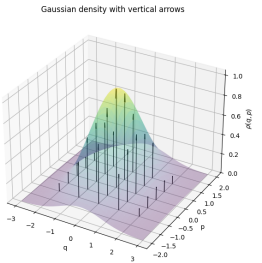


Discretization of the phase-space



$N = 2^n$ grid points per axis, D axes $\Rightarrow nD$ qubits

$$\rho(\boldsymbol{\phi}) \longmapsto |\rho\rangle = \sum_{\phi_1,\ldots,\phi_D} \frac{\rho(\boldsymbol{\phi})}{\|\rho\|} |\phi_1,\ldots,\phi_D\rangle$$



$$\partial_{\phi_\alpha} \longrightarrow \hat{\partial}_\alpha = \frac{1}{\Delta x_\alpha} \sum_{k=-p}^{p} a_k \, \hat{S}_\alpha^{k\,*}$$

$$\hat{S}_\alpha^k \, |\phi_1,\ldots,\phi_\alpha,\ldots,\phi_D\rangle = \quad |\phi_1,\ldots,\phi_\alpha + k\Delta x_\alpha,\ldots,\phi_D\rangle$$

* finite differences with periodic boundary conditions, error $O(\Delta x_\alpha^{2p})$

Define

$$-iH|\rho\rangle = -\sum_{\alpha,\beta,\gamma=1}^{D} C_{\alpha\beta\gamma}\, \hat{\phi}_\beta \hat{\phi}_\gamma\, \hat{\partial}_\alpha |\rho\rangle$$

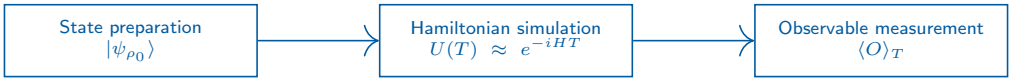
$$\boxed{\partial_t |\rho\rangle = -iH|\rho\rangle}$$

Schrödinger-type equation

For $\nabla_\phi \cdot f = 0$ and periodic boundary conditions, $\boxed{H^\dagger = H}$

Section 4

Quantum Numerical Scheme



Quantum State Preparation



We use a structured initial density:

$$\rho_0(\phi) \propto \exp\left[-\frac{\|\phi - \phi_0\|^2}{2\sigma^2}\right].$$

The corresponding quantum state is

$$|\psi_{\rho_0}\rangle = \sum_{\phi} \sqrt{\rho_0(\phi)}\,|\phi\rangle.$$

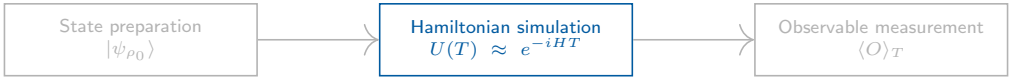
For a product Gaussian,

$$|\psi_{\rho_0}\rangle = \bigotimes_{\alpha=1}^{D} |\psi_{\sigma,\mu_\alpha}\rangle.$$

Efficient state preparation using the Walsh Series Loader

J. Zylberman and F. Debbasch, *Efficient quantum state preparation with Walsh series*, Phys. Rev. A **109**, 042401 (2024).

Trotterization



Decompose the generator coordinate-wise:

$$\mathcal{H} = \sum_{\alpha=1}^{D} \mathcal{H}_\alpha \xrightarrow{\text{1st order product formula}} e^{-i\Delta t\,\mathcal{H}} \simeq \prod_{\alpha=1}^{D} e^{-i\Delta t\,\mathcal{H}_\alpha}$$

Trotterization

State preparation $|\psi_{\rho_0}\rangle$ → **Hamiltonian simulation $U(T) \approx e^{-iHT}$** → Observable measurement $\langle O \rangle_T$

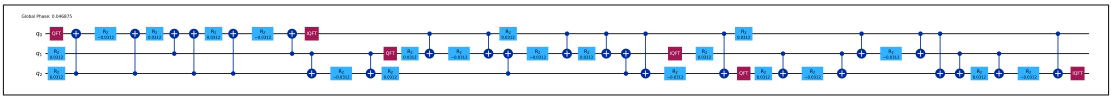
Decompose the generator coordinate-wise:

$$\mathcal{H} = \sum_{\alpha=1}^{D} \mathcal{H}_\alpha \xrightarrow{\text{1st order product formula}} e^{-i\Delta t\,\mathcal{H}} \simeq \prod_{\alpha=1}^{D} e^{-i\Delta t\,\mathcal{H}_\alpha}$$

For one coordinate,

$$e^{-i\Delta t\,\mathcal{H}_\alpha} = \mathrm{QFT}_\alpha^\dagger\, e^{-i\Delta t \left(\sum_{\beta,\gamma} C_{\alpha\beta\gamma} \hat{\phi}_\beta \hat{\phi}_\gamma \hat{\phi}_\alpha \right)} \mathrm{QFT}_\alpha$$

- QFT diagonalize derivative operator
- $\left[\mathrm{QFT}_\alpha, \hat{\hat{\phi}}_\alpha\right] = 0$



Only QFTs and $\mathcal{O}(Dn^3)$ $CNOT$ and R_z gates

What do we measure?



Main observable: mean position in phase space

For each coordinate ϕ_α:

$$\boxed{\langle \rho_\alpha \rangle_T = \langle \psi(T) | \widehat{\rho}_\alpha | \psi(T) \rangle}$$

For an n-qubit register encoding ϕ_α:

$$\widehat{\phi}_\alpha = \mathbb{I}^{\otimes(\alpha-1)} \otimes \widehat{X}_\alpha \otimes \mathbb{I}^{\otimes(D-\alpha)}, \qquad \boxed{\widehat{X} = \sum_{k=0}^{n-1} 2^{-k} \frac{I - Z_k}{2}}$$

What do we measure?



Main observable: mean position in phase space

For each coordinate ϕ_α:

$$\boxed{\langle \rho_\alpha \rangle_T = \langle \psi(T) | \widehat{\rho}_\alpha | \psi(T) \rangle}$$

For an n-qubit register encoding ϕ_α:

$$\widehat{\phi}_\alpha = \mathbb{I}^{\otimes(\alpha-1)} \otimes \widehat{X}_\alpha \otimes \mathbb{I}^{\otimes(D-\alpha)}, \qquad \boxed{\widehat{X} = \sum_{k=0}^{n-1} 2^{-k} \, \frac{I - Z_k}{2}}$$

More generally, any field observable can be expanded as a diagonal operator:

$$\widehat{O}_f = \sum_{\mathbf{X}} f(\boldsymbol{\phi}(\mathbf{X})) |\mathbf{X}\rangle\langle\mathbf{X}|, \qquad \boxed{\widehat{E} = \frac{1}{2} \sum_\alpha \widehat{\phi}_\alpha^2} \quad \text{and} \quad \boxed{\widehat{\Omega} = \frac{1}{2} \sum_\alpha k_\alpha^2 \widehat{\phi}_\alpha^2}$$

Section 5

Error Analysis

Approximation and error sources

For a $C_{\mathcal{O}}$-Lipschitz observable, $|\mathcal{O}(u) - \mathcal{O}(v)| \leq C_{\mathcal{O}} \|u - v\|_{L^2}$

$C_X = 1$ (Position)

$C_E \leq \sqrt{D}$ (Energy)

$$|\mathcal{O}(u) - \mathcal{O}(\tilde{u})| \leq \underbrace{C_0 \|u - \tilde{u}\|_{L^2}}_{\text{Spectral Truncation Error}} + \underbrace{|\mathcal{O}(\tilde{u}) - \mathcal{O}(\tilde{u}')|}_{\text{Liouville Error}} + \underbrace{|\mathcal{O}(\tilde{u}') - \mathcal{O}(\tilde{u}'')|}_{\text{Q.N.S. Error}}$$

Approximation and error sources

For a $C_{\mathcal{O}}$-Lipschitz observable, $|\mathcal{O}(u) - \mathcal{O}(v)| \leq C_{\mathcal{O}} \|u - v\|_{L^2}$

$C_X = 1$ (Position)

$C_E \leq \sqrt{D}$ (Energy)

$$|\mathcal{O}(u) - \mathcal{O}(\tilde{u})| \leq \underbrace{C_0 \|u - \tilde{u}\|_{L^2}}_{\text{Spectral Truncation Error}} + \underbrace{|\mathcal{O}(\tilde{u}) - \mathcal{O}(\tilde{u}')|}_{\text{Liouville Error}} + \underbrace{|\mathcal{O}(\tilde{u}') - \mathcal{O}(\tilde{u}'')|}_{\text{Q.N.S. Error}}$$

The term follow the error analysis of Zylberman et al. (2025):

$$|O_T - \langle \tilde{O}_T \rangle| \leq \underbrace{|O_T - {}_T\langle f | \hat{O} | f \rangle_T|}_{\text{Quadrature error}} + \underbrace{|\langle \tilde{O}_T \rangle - {}_T\left\langle \tilde{\tilde{f}}_\alpha \right| \hat{\tilde{O}} \left| \tilde{\tilde{f}}_\alpha \right\rangle_T|}_{\text{Statistical measurement error}} + \underbrace{\|\hat{O} - \hat{\tilde{O}}\|_2}_{\text{q.c. approximation}} + 2\|\hat{O}\|_2 \underbrace{\| \left| \tilde{\tilde{f}}_\alpha \right\rangle_T - \left| \tilde{f}_\alpha \right\rangle_T \|_{2,N}}_{\text{q.c. approximation}}$$

$$+ 2\|\hat{O}\|_2 \left(\underbrace{\| \left| \tilde{f}_\alpha \right\rangle_T - \left| \tilde{f} \right\rangle_T \|_{2,N}}_{\text{Product formula error}} + \underbrace{\| \left| \tilde{f} \right\rangle_T - |f\rangle_T \|_{2,N}}_{\text{Space discretization}} + \underbrace{\| \left| \tilde{f}_0 \right\rangle - |f_0\rangle \|_{2,N}}_{\text{Q.S.P. error}} \right).$$

Zylberman et al., 2025

Spectral Truncation error

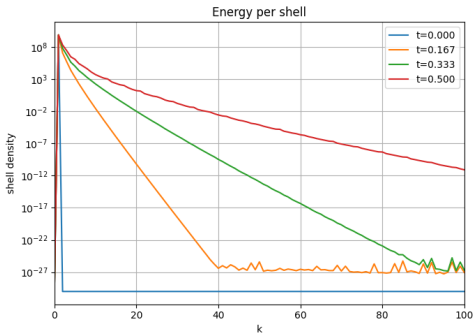


Figure 3: Energy per Fourier shell $E(k)$, $t = 0$ to 0.03

Convergence garanted !

$$u_0 \in H^s, \qquad \|u_0\|_\infty < \infty, \qquad \|\omega_0\|_\infty < \infty,$$

$$\Longrightarrow \sup_{t\in[0,T]} \left\| u^N(t) - u(t) \right\|_2 \leq \frac{C}{N^{s-1}}$$

Fourier–Galerkin approximation of the 2D Euler equations, Theorem 1.3 and Eq. (4.16)

Experiment

- Random initial condition, low modes only ($|\mathbf{k}| \leq 2$)
- Truncated dynamics, $|\mathbf{k}| < 150$: $O(10^5)$ modes

Liouville embedding error

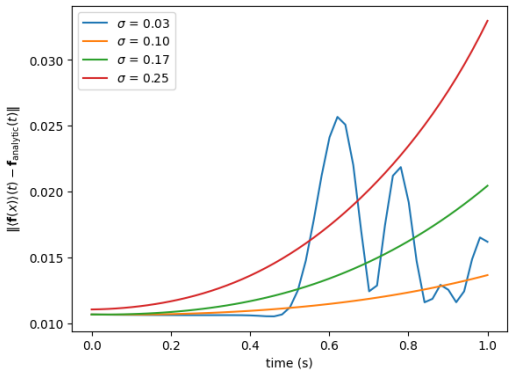


Figure 4: Error versus the exact three-mode ODE, for several σ

Experiment

- Three modes, packet at $(0.4, 0.4, 0.4)$
- Trotter: $\Delta t = 10^{-4}$, $N = 150$, $p = 2$

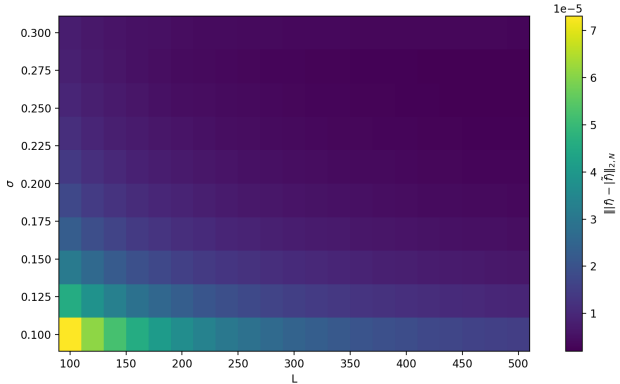
Trajectory can diverge exponentially

$$\|\phi(t) - \langle\phi(t)\rangle\| \leq e^{Kt} \|\phi(0) - \langle\phi(0)\rangle\|$$

To reach accuracy ϵ at time T,

$$\sigma_0 \lesssim \frac{\epsilon}{C_O} e^{-KT} \implies n \gtrsim \frac{KT}{\log 2} + \log_2 \frac{C_O}{\epsilon}$$

Trotterization Error



Prefactor scaling

$$\epsilon_{\text{Trotter}} \lesssim \alpha_s' \frac{T^2}{L}$$

$$\alpha_s' = \mathcal{O}\left(\frac{\|\partial_{x_m} f_0\|_{L^2}}{\|f_0\|_{L^2}} \right)$$

$\sigma \downarrow \quad \Rightarrow \quad$ better localization $\quad \Rightarrow \quad$ larger gradients $\quad \Rightarrow \quad$ larger Trotter prefactor

Section 6

Numerical Experiment

A controlled benchmark: the three-wave subsystem

We restrict the spectrally truncated Euler dynamics to Lorenz's maximal simplification:

$$A = b_{(1,0)}, \qquad F = b_{(0,1)}, \qquad G = b_{(1,1)} = -b_{(1,-1)}.$$

The dynamics closes:

$$\boxed{\dot{A} = aFG, \qquad \dot{F} = bAG, \qquad \dot{G} = cAF.}$$

- It is a closed subsystem of the spectrally truncated Euler dynamics.
- It retains the elementary three-wave interactions of the full system.
- It has conserved energy and enstrophy, together with an analytic elliptic-function solution.

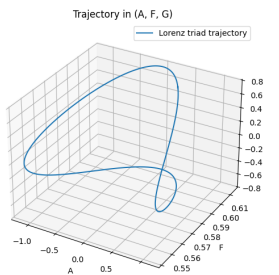


Figure 5: The three-wave subsystem is a low-dimensional testbed for the Liouville construction.

The mean of the Liouville density tracks the trajectory

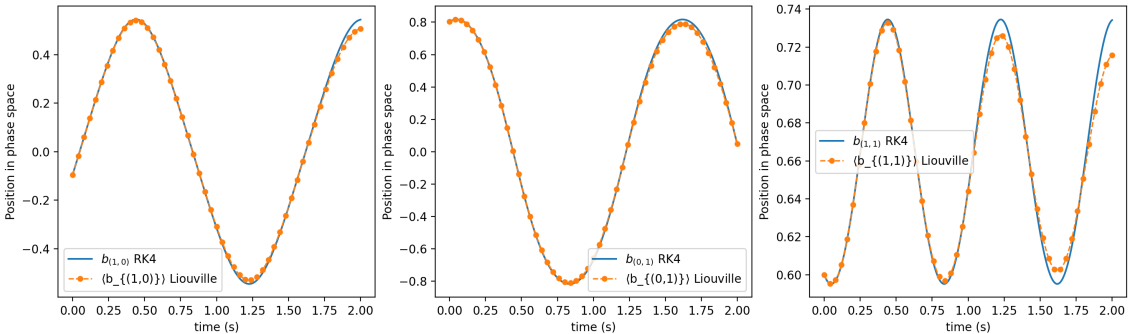


Figure 6: Reconstructed trajectory from the Liouville density (blue) versus the reference trajectory (orange). The initial Gaussian packet is centered at $(A, F, G) = (-0.1, 0.8, 0.6)$ with width $\sigma = 0.03$. The Trotter evolution uses $L = 2000$ steps over $T = 2$.

Tracking the trajectory in phase-space

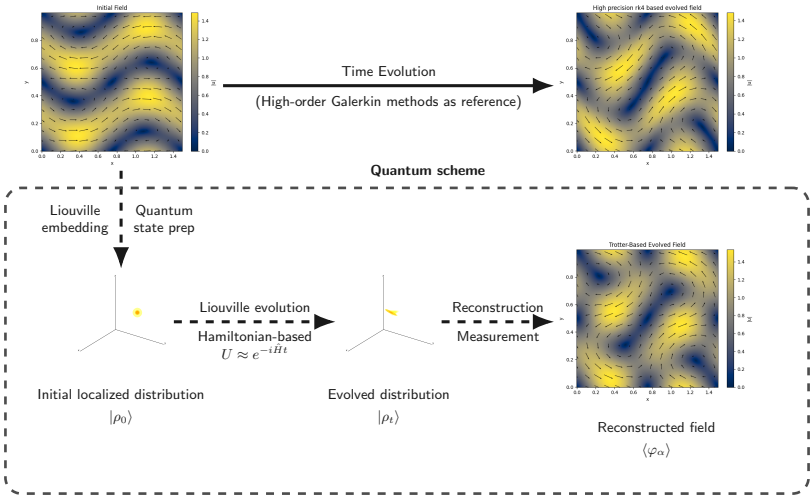


Figure 7: Liouville-based simulation on a three-mode subsystem of the spectrally truncated Euler dynamics. Top: initial field and 100-mode reference evolution. Bottom: Gaussian packet centered at $(A, F, G) = (-0.1, 0.8, 0.8)$, $\sigma = 0.04$, its 1000-step

Conclusion & Perspectives

We did not make the fluid dynamics linear.

We changed the object we evolve.

What we did

- Quantum scheme for ideal fluids
- Liouville $\rightarrow$ Hamiltonian simulation
- Numerical validation

Error analysis

- Error decomposition
- Spectral & phase-space discretization
- Product-formula error

What's next?

- Understand Liouville errors & closure
- More efficient Hamiltonian simulation
- Investigate quantum advantage

Thank you

Questions?

Quantum simulation of ideal fluids

Martin Pujol
CERFACS

Complexity of the Q.N.S : where the real cost sits

The total cost is naturally decomposed as

$$\boxed{C_{\text{total}} = C_{\text{prep}} + C_{\text{evol}} + C_{\text{obs}}}$$

per execution of the circuit.
For first-order Trotterization, the manuscript gives

$$L = O\left(\frac{T^2}{\epsilon}\right)$$

and

$$C_{\text{evol}} = O\left(\frac{D^3 T^2}{\epsilon^2}\left(C_{\text{diag}} + 2C_{\text{QFT}}\right)\right).$$

With

$$C_{\text{diag}} = O(Dn^3), \qquad C_{\text{QFT}} = O(n^2),$$

this becomes

$$\boxed{C_{\text{evol}} = O\left(\frac{D^4 T^2 n^3}{\epsilon^2}\right)}$$

up to implementation-dependent constants.

Backup: Time dependence of the spectral bound

For $u_0 \in H^s(\mathbb{T}^2)$, $s > 2$, the 2D Euler solution satisfies

$$\boxed{\sup_{t\in[0,T]} \|u(t)\|_{H^s} \leq C(T, \|u_0\|_{H^s})}$$

The time dependence hidden in C can be severe:

$$\boxed{\|\nabla\omega(t)\|_\infty \text{ can grow double exponentially in time.}}$$

Fourier–Galerkin approximation of the 2D Euler equations, Theorem 1.3 and Eq. (4.16).

S. A. Denisov, *Double exponential growth of the vorticity gradient for the two-dimensional Euler equation*, Proc. Amer. Math. Soc. **143**(3), 1199–1210 (2015).

Backup : From Clebsch variables to the vorticity formulation

Clebsch formulation

$$\mathbf{u} = \nabla\phi + \alpha\nabla\beta$$

$$(\rho, \phi), \qquad (\rho\alpha, \beta)$$

canonical conjugate pairs

$$\delta S = 0 \quad \Longleftrightarrow \quad \begin{cases} \partial_t \rho + \nabla\cdot(\rho\mathbf{u}) = 0, \\ \partial_t \mathbf{u} + (\mathbf{u}\cdot\nabla)\mathbf{u} = -\dfrac{1}{\rho}\nabla p. \end{cases}$$

compressible Euler

Incompressible reduction

$$\nabla\cdot\mathbf{u} = 0 \qquad \Longrightarrow \qquad \text{Symetry reduction}$$

canonical $\longrightarrow$ degenerate Poisson structure

$$\mathbf{u} = \nabla^{\perp}\psi, \qquad \omega = \Delta\psi$$

$$\boxed{\partial_t \omega + [\psi, \omega] = 0}$$

Spectral Truncation



Expand the vorticity field on $\mathbb{T}^2$:

$$\omega^M(\mathbf{x},t) = \sqrt{\tfrac{2}{V}} \sum_{|\mathbf{k}|<M} \left[a_{\mathbf{k}}(t)\ \cos(\mathbf{k}\cdot\mathbf{x}) + b_{\mathbf{k}}(t)\sin(\mathbf{k}\cdot\mathbf{x})\right]$$

Spectral Truncation



Expand the vorticity field on $\mathbb{T}^2$:

$$\omega^M(\mathbf{x},t) = \sqrt{\tfrac{2}{V}} \sum_{|\mathbf{k}|<M} \left[a_{\mathbf{k}}(t)\ \cos(\mathbf{k}\cdot\mathbf{x}) + b_{\mathbf{k}}(t)\sin(\mathbf{k}\cdot\mathbf{x})\right]$$

Mode Dynamics

$$\dot{a}_{\mathbf{p}} = \left(\tfrac{2}{V}\right)^{1/2} \sum_{\mathbf{k}} \frac{\mathbf{k}\wedge\mathbf{p}}{|\mathbf{k}||\mathbf{p}|}\left[\frac{\mathbf{p}\cdot(\mathbf{p}-\mathbf{k})}{|\mathbf{p}-\mathbf{k}|}\left(a_{\mathbf{k}}b_{\mathbf{p}-\mathbf{k}} + b_{\mathbf{k}}a_{\mathbf{k}-\mathbf{p}} - b_{\mathbf{k}}a_{\mathbf{p}-\mathbf{k}}\right) - \frac{\mathbf{p}\cdot(\mathbf{p}+\mathbf{k})}{|\mathbf{p}+\mathbf{k}|}\, a_{\mathbf{k}}b_{\mathbf{p}+\mathbf{k}}\right],$$

$$\dot{b}_{\mathbf{p}} = \left(\tfrac{2}{V}\right)^{1/2} \sum_{\mathbf{k}} \frac{\mathbf{k}\wedge\mathbf{p}}{|\mathbf{k}||\mathbf{p}|}\left[\frac{\mathbf{p}\cdot(\mathbf{p}-\mathbf{k})}{|\mathbf{p}-\mathbf{k}|}\left(b_{\mathbf{k}}b_{\mathbf{p}-\mathbf{k}} + a_{\mathbf{k}}a_{\mathbf{k}-\mathbf{p}} - a_{\mathbf{k}}a_{\mathbf{p}-\mathbf{k}}\right) - \frac{\mathbf{p}\cdot(\mathbf{p}+\mathbf{k})}{|\mathbf{p}+\mathbf{k}|}\, b_{\mathbf{k}}b_{\mathbf{p}+\mathbf{k}}\right].$$

Backup — three-wave equations

The explicit system used in the benchmark is

$$\dot{A} = aFG, \qquad \dot{F} = bAG, \qquad \dot{G} = cAF.$$

For the geometry used in the manuscript, with

$$k = \frac{2\pi}{L_x}, \qquad \ell = \frac{2\pi}{L_y},$$

the coupling coefficients are

$$a = \sqrt{\frac{2k}{\ell}}\,\frac{k}{\sqrt{k^2+\ell^2}},$$

$$b = -\sqrt{\frac{2k}{\ell}}\,\frac{\ell}{\sqrt{k^2+\ell^2}},$$

$$c = -\sqrt{\frac{k}{2\ell}}\,\frac{k^2-\ell^2}{\sqrt{k^2+\ell^2}}.$$

The conserved quantities are

$$E = A^2 + F^2 + 2G^2,$$

$$Q = k^2A^2 + \ell^2F^2 + 2(k^2+\ell^2)G^2$$

Space-Discretization error

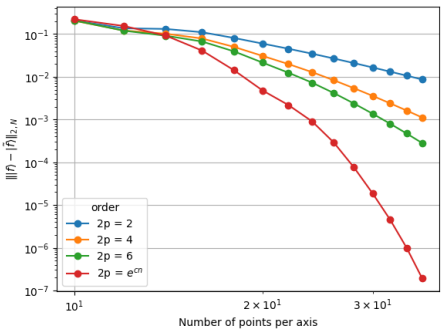


Figure 8:

Spectral derivatives converge superpolynomially

$$f \in C^p \qquad \Longrightarrow \qquad \left| \partial_x f(x_j) - \left(\widehat{\partial_x} f \right)^j \right| \lesssim N^{2-p}$$

Experiment

- Gaussian packet: $(A_0, F_0, G_0) = (0.4, 0.4, 0.4)$, $\sigma = 0.2$
- Exact Lorenz inverse-flow reference
- $N = 200$ grid points per phase-space direction
- Error: $\|\rho_{\text{ref}} - \rho_{\text{num},p}\|_{2,N}$

Backup Properties of the truncated system



Mode Dynamics

$$\dot{a}_{\mathbf{p}} = \left(\tfrac{2}{V}\right)^{1/2} \sum_{\mathbf{k}} \frac{\mathbf{k}\wedge\mathbf{p}}{|\mathbf{k}||\mathbf{p}|}\left[\frac{\mathbf{p}\cdot(\mathbf{p}-\mathbf{k})}{|\mathbf{p}-\mathbf{k}|}\left(a_{\mathbf{k}}b_{\mathbf{p}-\mathbf{k}} + b_{\mathbf{k}}a_{\mathbf{k}-\mathbf{p}} - b_{\mathbf{k}}a_{\mathbf{p}-\mathbf{k}}\right) - \frac{\mathbf{p}\cdot(\mathbf{p}+\mathbf{k})}{|\mathbf{p}+\mathbf{k}|}\, a_{\mathbf{k}}b_{\mathbf{p}+\mathbf{k}}\right],$$

$$\dot{b}_{\mathbf{p}} = \left(\tfrac{2}{V}\right)^{1/2} \sum_{\mathbf{k}} \frac{\mathbf{k}\wedge\mathbf{p}}{|\mathbf{k}||\mathbf{p}|}\left[\frac{\mathbf{p}\cdot(\mathbf{p}-\mathbf{k})}{|\mathbf{p}-\mathbf{k}|}\left(b_{\mathbf{k}}b_{\mathbf{p}-\mathbf{k}} + a_{\mathbf{k}}a_{\mathbf{k}-\mathbf{p}} - a_{\mathbf{k}}a_{\mathbf{p}-\mathbf{k}}\right) - \frac{\mathbf{p}\cdot(\mathbf{p}+\mathbf{k})}{|\mathbf{p}+\mathbf{k}|}\, b_{\mathbf{k}}b_{\mathbf{p}+\mathbf{k}}\right].$$

Backup Properties of the truncated system



Mode Dynamics

$$\dot{a}_{\mathbf{p}} = \left(\tfrac{2}{V}\right)^{1/2} \sum_{\mathbf{k}} \frac{\mathbf{k}\wedge\mathbf{p}}{|\mathbf{k}||\mathbf{p}|}\left[\frac{\mathbf{p}\cdot(\mathbf{p}-\mathbf{k})}{|\mathbf{p}-\mathbf{k}|}\left(a_{\mathbf{k}}b_{\mathbf{p}-\mathbf{k}} + b_{\mathbf{k}}a_{\mathbf{k}-\mathbf{p}} - b_{\mathbf{k}}a_{\mathbf{p}-\mathbf{k}}\right) - \frac{\mathbf{p}\cdot(\mathbf{p}+\mathbf{k})}{|\mathbf{p}+\mathbf{k}|}\, a_{\mathbf{k}}b_{\mathbf{p}+\mathbf{k}}\right],$$

$$\dot{b}_{\mathbf{p}} = \left(\tfrac{2}{V}\right)^{1/2} \sum_{\mathbf{k}} \frac{\mathbf{k}\wedge\mathbf{p}}{|\mathbf{k}||\mathbf{p}|}\left[\frac{\mathbf{p}\cdot(\mathbf{p}-\mathbf{k})}{|\mathbf{p}-\mathbf{k}|}\left(b_{\mathbf{k}}b_{\mathbf{p}-\mathbf{k}} + a_{\mathbf{k}}a_{\mathbf{k}-\mathbf{p}} - a_{\mathbf{k}}a_{\mathbf{p}-\mathbf{k}}\right) - \frac{\mathbf{p}\cdot(\mathbf{p}+\mathbf{k})}{|\mathbf{p}+\mathbf{k}|}\, b_{\mathbf{k}}b_{\mathbf{p}+\mathbf{k}}\right].$$

Stack the coefficients in one vector, with $D = O(N^2)$:

$$\boldsymbol{\phi} = \begin{pmatrix} a_{(0,-N)} \\ \vdots \\ a_{(N,N)} \\ b_{(0,-N)} \\ \vdots \\ b_{(N,N)} \end{pmatrix} \xrightarrow{\text{quadratic flow}} \boxed{\dot{\phi}_\alpha = \sum_{\beta,\gamma=1}^{D} C_{\alpha\beta\gamma}\,\phi_\beta\phi_\gamma}$$

Backup Properties of the truncated system



Mode Dynamics

$$\dot{a}_{\mathbf{p}} = \left(\tfrac{2}{V}\right)^{1/2} \sum_{\mathbf{k}} \frac{\mathbf{k}\wedge\mathbf{p}}{|\mathbf{k}||\mathbf{p}|}\left[\frac{\mathbf{p}\cdot(\mathbf{p}-\mathbf{k})}{|\mathbf{p}-\mathbf{k}|}\left(a_{\mathbf{k}}b_{\mathbf{p}-\mathbf{k}} + b_{\mathbf{k}}a_{\mathbf{k}-\mathbf{p}} - b_{\mathbf{k}}a_{\mathbf{p}-\mathbf{k}}\right) - \frac{\mathbf{p}\cdot(\mathbf{p}+\mathbf{k})}{|\mathbf{p}+\mathbf{k}|}\, a_{\mathbf{k}}b_{\mathbf{p}+\mathbf{k}}\right],$$

$$\dot{b}_{\mathbf{p}} = \left(\tfrac{2}{V}\right)^{1/2} \sum_{\mathbf{k}} \frac{\mathbf{k}\wedge\mathbf{p}}{|\mathbf{k}||\mathbf{p}|}\left[\frac{\mathbf{p}\cdot(\mathbf{p}-\mathbf{k})}{|\mathbf{p}-\mathbf{k}|}\left(b_{\mathbf{k}}b_{\mathbf{p}-\mathbf{k}} + a_{\mathbf{k}}a_{\mathbf{k}-\mathbf{p}} - a_{\mathbf{k}}a_{\mathbf{p}-\mathbf{k}}\right) - \frac{\mathbf{p}\cdot(\mathbf{p}+\mathbf{k})}{|\mathbf{p}+\mathbf{k}|}\, b_{\mathbf{k}}b_{\mathbf{p}+\mathbf{k}}\right].$$

Stack the coefficients in one vector, with $D = O(N^2)$:

$$\boldsymbol{\phi} = \begin{pmatrix} a_{(0,-N)} \\ \vdots \\ a_{(N,N)} \\ b_{(0,-N)} \\ \vdots \\ b_{(N,N)} \end{pmatrix} \xrightarrow{\text{quadratic flow}} \boxed{\dot{\phi}_\alpha = \sum_{\beta,\gamma=1}^{D} C_{\alpha\beta\gamma}\,\phi_\beta\phi_\gamma}$$

- Antisymmetry of $C \Rightarrow \dot{E}$
- Hard incompressibility constraint: $\dfrac{\partial\dot{\phi}_\alpha}{\partial\phi_\alpha} = 0 \;\Rightarrow\; \sum_{\alpha=1}^{D} \dfrac{\partial\dot{\phi}_\alpha}{\partial\phi_\alpha} = 0$

Backup — Gaussian localization and instability

For an observable O with Lipschitz constant C_O,

$$|O(\phi(t)) - \mathbb{E}_{\rho_t}[O]| \lesssim C_O \sigma_0 e^{Kt}.$$

Hence

$$\sigma_0 \lesssim \frac{\epsilon}{C_O} e^{-KT}.$$

With

$$\Delta\phi = O(2^{-n}),$$

we obtain

$$n \gtrsim \frac{KT}{\log 2} + \log_2 \frac{C_O}{\epsilon}.$$

Thus the number of grid points required for fixed-accuracy trajectory tracking grows exponentially with time, even though the number of qubits per coordinate grows only linearly.

Backup — evolution cost

The proposed first-order product formula has

$$L = O\left(\frac{T^2}{\epsilon}\right)$$

steps in the baseline analysis.
The evolution cost is

$$C_{\mathrm{evol}} = O\left[\frac{D^3 T^2}{\epsilon^2}\left(C_{\mathrm{diag}} + 2C_{\mathrm{QFT}}\right)\right].$$

Using

$$C_{\mathrm{diag}} = O(Dn^3), \qquad C_{\mathrm{QFT}} = O(n^2),$$

gives

$$C_{\mathrm{evol}} = O\left(\frac{D^4 T^2 n^3}{\epsilon^2}\right).$$

This scaling should be presented as the resource estimate of the current construction, not as a claim that the current Trotter implementation is optimal.